



J. Serb. Chem. Soc. 89 (10) 1323–1336 (2024)
JSCS–5790

Electrical, optical and structural characterization of interfaces containing poly(3-alkylthiophenes) (P3ATs) and polydiphenylamine on ITO/TiO₂: Interaction between P3ATs polymeric segments and TiO₂

MAYARA MASAE KUBOTA¹, RICARDO VIGNOTO FERNANDES²
and HENRIQUE DE SANTANA^{1*}

¹Departamento de Química, CCE, Universidade Estadual de Londrina, Londrina, PR 86051-990, Brazil and ²Departamento de Física, CCE, Universidade Estadual de Londrina, Londrina, PR 86051-990, Brazil

(Received 25 November 2023, revised 24 January, accepted 3 March 2024)

Abstract: With the aim of studying the use of conjugated polymers poly(3-methylthiophene) (P3MT), poly(3-hexylthiophene) (P3HT) and polydiphenylamine (PDPA) in order to produce the active layer of inverted organic solar cells forming the interface with TiO₂ and also to help shed light on the optical and electronic properties applied to develop this technology, the interfaces between films containing P3MT, P3HT and PDPA on the indium tin oxide (ITO) electrode were electrochemically prepared, after chemically depositing a film of TiO₂. The systems under investigation were designated ITO/TiO₂/P3MT, ITO/TiO₂/PDPA/P3MT, ITO/TiO₂/PDPA, ITO/TiO₂/P3HT and ITO/TiO₂/PDPA/P3HT and characterized by Raman techniques (spectroscopy and microscopy), electrochemical impedance spectroscopy (EIS) and photoluminescence (PL). In this study, the aromatic, semiquinone and quinone segments in the polymer matrices of P3ATs and PDPA at these interfaces were monitored and characterized by comparison with films of their homopolymers by means of Raman spectroscopy and EIS. The Raman imaging demonstrates that the P3MT film can be incorporated into the titanium oxide crystalline lattice. The systems containing P3MT or P3HT were found to strongly interact with the TiO₂, stabilizing the P3AT radical cation segments and the presence of PDPA destabilized this interaction. These findings were complemented by the low-temperature (15 K) PL spectra, revealing a reduction in the intensity and displacement of the band associated with the radical cation emission, observed in the absence of TiO₂ in the system under investigation.

Keywords: film incorporated; interaction; Raman; EIS; organic photovoltaic cells.

* Corresponding author. E-mail: hensan@uel.br
<https://doi.org/10.2298/JSC231125024K>



INTRODUCTION

Over the last few decades, the attempts have been made to incorporate organic solar cells as a possible renewable, clean, sustainable and low-cost energy source.^{1,2} In this context, the organic semiconductor polymers play a central role, since they exhibit a number of advantages over inorganic materials, *i.e.*, they are low-cost, lightweight and flexible.¹ However, despite the numerous advantages of these polymers, they are still not commercially available because they are still not very efficient in terms of solar energy conversion into electrical energy. For this reason, it is of key importance to study and characterize new materials to make up the photoactive layer of the device in order to improve the energy conversion rate.¹⁻⁴

Most solar cells based on conjugated polymers are manufactured using conventional architecture, designed in layers made up of a transparent conducting substrate (ITO), a hole-transporting layer (anode), a photoactive layer containing an electron donor polymer, a photoactive layer containing an electron donor polymer and electron acceptor compound and a metal electrode with high work function to improve electron transportation (cathode). However, in this configuration some compounds such as poly(3,4-ethylenedioxythiophene) : poly(styrene sulfonate), generally used in the anode, cause instability at the interface of the photoactive layer due to ITO corrosion.^{1,2} To improve the interface stability and prevent device degradation, one alternative would be to use an inverted configuration in which the ITO acts as the cathode and a high work function metal as the anode, affording greater device stability.¹⁻³ The use of a thin layer of TiO₂ as an electron selective layer is very effective in inverted solar cells.²

For the photoactive layer, the polymer mix system currently under investigation is based on P3HT and fullerene [6,6]-phenyl-C₆₁-butyric acid methyl ester (PCBM). This polymer mix boosted efficiency by up to 5 % and interfaces incorporating this material have been fairly well investigated in order to improve its properties. The use of optical and spectroscopic techniques in the structural characterization of these systems has helped to improve our understanding of the emission and charge transporting processes.^{2,5-7}

The studies aimed at the structural characterization using Raman spectroscopy and EIS on systems containing PDPA, P3HT and P3MT to form the active layer on platinum and ITO and their comparison with the monomer structures have shown variations in charge transfer resistance processes and linked them to the equilibrium displacements among aromatic, radical cation and dication segments along the polymer matrix of the materials produced.⁸

With the aim of evaluating the interfaces forming the active layer and examine whether their properties are suitable for the inverted organic solar cell applications, ITO/TiO₂/P3MT, ITO/TiO₂/PDPA/P3MT, ITO/TiO₂/PDPA, ITO/TiO₂/

/P3HT and ITO/TiO₂/PDPA/P3HT systems were prepared using chemical and electrochemical techniques and characterized by Raman spectroscopy, EIS and PL.

EXPERIMENTAL

Reagents

3-hexylthiophene monomer (C₁₀H₁₆S), 3-methylthiophene (C₅H₆S) and diphenylamine ((C₆H₅)₂NH) were supplied by Sigma–Aldrich and used as received. The support electrolyte was lithium perchlorate (LiClO₄, 99 % pure; AcrosOrganics) and the solvent was acetonitrile (ACN, high-performance liquid chromatography (HPLC) grade, 99.5 % pure; JT Baker).

Electrochemical synthesis and cyclic voltammetry

PDPA was synthesized by cyclic voltammetry, varying the potential between 0.60 and 1.20 V in steps of 100 mV s⁻¹ in a solution of 0.10 mol L⁻¹ DPA in LiClO₄–ACN onto ITO electrodes for 50 cycles at 22 °C. The electrode incorporating the PDPA film was removed at a potential of 1.2 V and kept at ambient temperature.

P3HT and P3MT films were synthesized electrochemically by chronoamperometry, applying the potentials of 1.80 and 1.65 V to the P3HT and P3MT, respectively, in a solution of 3-hexylthiophene and 3-methylthiophene monomers at concentrations of 0.04 and 0.035 mol L⁻¹ in LiClO₄–ACN respectively. The temperature was kept constant at 22 °C during the synthesis. The electrode with P3HT and P3MT films were removed from the solution at a potential of 1.65 or 1.80 V and kept at ambient temperature.

To prepare a layer of P3HT on the substrate/PDPA interphase, PDPA was initially synthesized on the substrate and the P3HT or P3MT films subsequently synthesized on this material under the aforementioned synthesis conditions. After the deposition on the electrodes, the films were kept at ambient temperature pending characterization after the analysis times stated herein had elapsed.

Both chronoamperometry and cyclic voltammetry were performed using a potentiostat/galvanostat (Autolab PGSTAT 302 N) coupled to a microcomputer running NOVA 1.8 software. The auxiliary electrode was a platinum plate of an area of 0.50 cm². The potentials were determined with reference to Ag/AgCl in a Luggin capillary in a 0.10 mol L⁻¹ solution of lithium perchlorate in acetonitrile (LiClO₄–ACN).

Synthesis of TiO₂ films

The TiO₂ sol was synthesized using a method described by Hoffmann *et al.*⁹ and Nazeeruddin *et al.*¹⁰ A solution consisting of 0.39 mL NH₄OH, 0.34 mL H₂O₂, 10 mL H₂O and 0.70 g TiO₂ was dispersed in a 25 mL beaker and the gel formed was heated to 75 °C under magnetic agitation for 2 h. To increase the gel fluidity, three drops of Triton X-100 and seven drops of acetylacetone were added to the solution. The TiO₂ thin film was prepared using a painter's method on 1.2 cm² of Ti. It was dried at 100 for 10 min and calcined at 500 °C for 2 h. The films were then cooled to ambient temperature.

Raman spectroscopy and microscopy

Ex situ Raman spectra were obtained using a portable Raman spectrometer (Advantage532®, DeltaNu) excited at 532 nm, with a resolution of 8 cm⁻¹. DeltaNu NuSpec software and baseline resources were used to remove background fluorescence.

Raman imaging was obtained using an alpha300+ WITec® confocal Raman microscope system (excitation at 532 nm), with a ZEISS 50× lens.

Electrochemical impedance spectroscopy (EIS)

The impedance diagrams were obtained using a potentiostat (AutoLab PGSTAT 302 N) with the FRAM32 impedance module and varying the frequency from 100 kHz to 0.01 Hz. The open circuit stabilization potentials (E_{OC}) were reached when the E_{OC} remained constant (± 5 mV) for 30 min, the time necessary to reach the stationary state.

Photoluminescence (PL)

PL measurements were taken in a helium closed-cycle cryostat at a temperature of 15 K. A 15 mW, 405 nm laser was used (Laserline, FDA Laser Power supply). The emissions from the sample were captured using a 5.5 cm lens and two colour filters (Schott GG435 and Edmund GG435). The detection was done by an Ocean Optics USB4000 mini-spectrometer.

RESULTS AND DISCUSSION

To monitor the polymer matrix in terms of thiophene, aromatic and quinone rings (radical cation and dication segments) were stabilized at the interfaces between the TiO_2 and P3HT or P3MT, *i.e.*, at the ITO/ TiO_2 /P3HT and ITO/ TiO_2 /P3MT interfaces and we obtained *ex situ* Raman spectra of these systems at different times after the electrochemical synthesis.

Fig. 1 shows the Raman spectra for the ITO/ TiO_2 /P3HT system obtained at different post-synthesis times. After the synthesis (Fig. 1a) we observed low intensity bands at 1373 cm^{-1} characteristic of C–C stretching of the ring and around 1450 cm^{-1} characteristic of symmetric C=C stretching of the thiophene ring.¹¹ As time progressed the latter band was displaced from $1450\text{--}1454\text{ cm}^{-1}$ and the spectrum exhibited an improved signal/noise ratio.

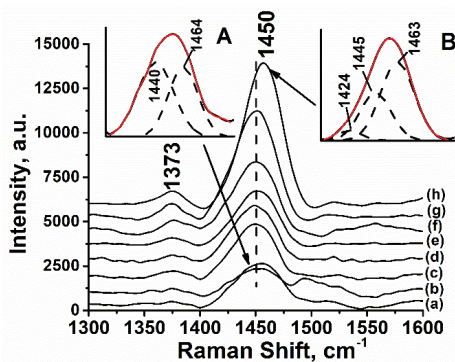


Fig. 1. Raman spectrum of the ITO/ TiO_2 /P3HT system. Post-synthesis times of: a) 0, b) 1, c) 5, d) 10, e) 15, f) 24, g) 30 and h) 97 h were applied at excitation radiation of 532 nm. Inset: deconvoluted Raman spectra of the ITO/ TiO_2 /P3HT system after: A) 0 and B) 97 h.

The elongated band centred at 1450 cm^{-1} is associated with the contributing radical cation, dication and aromatic segments of the thiophene ring, which coexisted in the polymer matrix of the P3HT after electrochemical synthesis.^{12,13} However, this involved deconvoluting this band in order to observe the presence of each of these segments.

As shown in the inset A of Fig. 1, shortly after the synthesis of the ITO/ TiO_2 /P3HT system, the deconvolution is accompanied by bands at 1440 and 1464 cm^{-1} ,

respectively, associated with the dication and radical cation segments of the thiophene ring. Inset B shows that after keeping the film under ambient conditions for 97 h, the deconvolution enabled us to observe the frequencies at 1424, 1445 and 1463 cm⁻¹, respectively, related to the aromatic, dication and radical cation segments of the thiophene ring.⁸ The deconvolution of the band associated with the radical cation segment was intensified by the deconvolution compared to the system shortly after synthesis.

These findings can be compared to those obtained by Kubota *et al.*,⁸ in which, under the same electrochemical synthesis conditions, the deposition of P3HT on the ITO conductive substrate was observed. At this interface, the stabilization of the radical cation was not as pronounced as at the interface with TiO₂, leading us to conclude that the TiO₂ interacts more strongly with the polymer material in order to stabilize the radical cation segments of the P3HT.

To complement the results obtained using Raman spectroscopy, the impedance magnitude and the Bode-phase diagrams were plotted based on the data obtained by EIS for the ITO/TiO₂ and ITO/TiO₂/P3HT systems in 0.100 mol L⁻¹ LiClO₄-ACN. EIS measurements were taken at an open circuit potential (OCP) and monitored at the same post-synthesis times as those applied to the Raman spectra after deposition of the film on the ITO/TiO₂ electrode. The intensity magnitude diagram is a piece of data that should be plotted together with the Bode-phase diagram to support the latter results; thus, only Bode-phase's data were commented on.

Fig. 2a and b show the impedance magnitude and the Bode-phase diagrams plotted for the ITO/TiO₂/P3HT system. The low-frequency phase maxima were observed at around 0.02, 0.04 and 0.08 Hz (Fig. 2b) and related to the charge transfer processes at the interface. In the study carried out by Kubota *et al.*,⁸ EIS measurements over time showed that, at times of up to 5 h, the two phase maximum at low and high frequencies were observed and became unstable after this time had elapsed. The elongated phase maximum at high frequency was predominant, indicating the stability of the dication segment after 48 h had elapsed.

In the results obtained in the presence of TiO₂, the low-frequency phase maximum could indicate that the charge transfer by conduction is primarily polaronic. However, instability in the system was observed, mainly after 1, 10 and 24 h, with a drastic reduction in the intensity of the phase angle at ~0.02 Hz. This effect resulted in more intense phase angles at frequencies of ~0.04 and ~0.08 Hz, probably due to a drop in the contribution of radical cation segments compared to the dication segments, thus increasing the bipolaronic conduction of the material.⁵ This natural deprotonation effect, involving the equilibrium between the number of radical cation and dication segments in the polymer matrix, could be considered responsible for the instability observed. However, due to the possibility of a strong interaction between TiO₂ and the P3HT system, the radical cation

segments could be primarily undergoing restabilization after a period of 30 h, as observed by the predominance of the stabilized phase maximum at low frequency (~ 0.02 Hz). Therefore, this result could be considered contingent on those previously obtained by the Raman spectra and that show higher intensity in the band associated with the radical cation segments on the same timescale.

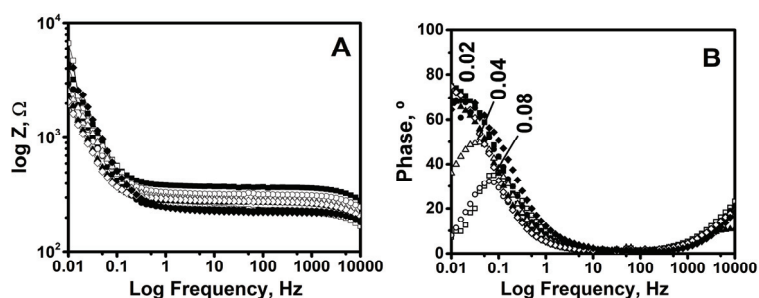


Fig. 2. a) Impedance magnitude and b) Bode-phase diagrams at open circuit potential and constant temperature of 22 °C for the ITO/TiO₂/P3HT system. Post-synthesis analysis times were: 0 (solid square), 1 (empty square), 5 (solid circle), 10 (empty circle), 15 (solid triangle), 24 (empty triangle), 30 (empty lozenge) and 97 h (solid lozenge) after electrochemical synthesis.

To confirm the results obtained previously, the diagrams of the impedance magnitude (Fig. S-1A of the Supplementary material to this paper) and the phase angle as a function of the frequency (Fig. S-1B) of the ITO/TiO₂ system were presented.

Fig. S-1B shows the Bode-phase diagram plotted for the ITO/TiO₂ system, showing the presence of a low-frequency phase maximum around 0.13 Hz and a high-frequency phase maximum around 14.70 Hz. This result indicates that the low-frequency phase maximum of TiO₂ has a strong interaction with the low-frequency phase maximum of P3MT, since in the ITO/P3MT system there are two phases, one in the low and one in the high frequency, however, in the ITO/TiO₂/P3MT system there is only the appearance of the low-frequency phase maximum, indicating the high amount of cation radical as seen in the data obtained by the Raman and IES techniques.

Fig. 3 shows the Raman spectra for the ITO/TiO₂/P3MT system, obtained at different time intervals. After synthesis, the Raman spectrum shows the characteristic frequencies of the P3MT thiophene ring at 1204 cm⁻¹, attributed to the C–C interring stretching, at 1335 cm⁻¹ attributed to symmetric inter-ring C–C stretching, the band at 1423 cm⁻¹, generally attributed to symmetric C=C stretching of the thiophene ring and the band at 1518 cm⁻¹ characteristic of asymmetric C=C stretching of the thiophene ring.¹⁴

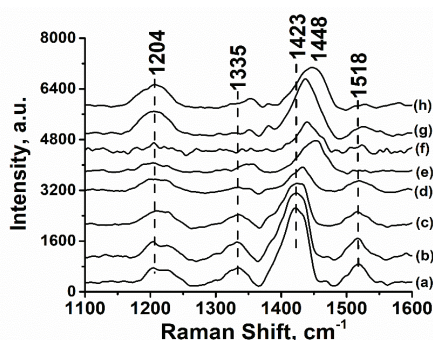


Fig. 3. Raman spectra for the ITO/TiO₂/P3MT system. Post-synthesis analysis times were: a) 0, b) 1, c) 5 d) 10, e) 15, f) 24, g) 30 and h) 97 h at excitation of 532 nm.

These results are comparable to those in De Lima *et al.*,⁸ in which, under the same electrochemical synthesis conditions, P3MT deposition on ITO was investigated. After synthesis, the frequencies were observed at 1205, 1331, 1480 and 1515 cm⁻¹. Of these bands, only the band at 1480 cm⁻¹, attributed to the radical cation segment of the P3MT, was observed at 1423 cm⁻¹ in the spectrum for the system containing TiO₂ at the interface with P3MT.

After 15 h, the band at 1423 cm⁻¹ was shifted to 1448 cm⁻¹, quite close to that observed by De Lima *et al.*,⁷ and after 15 h to 1457 cm⁻¹.

The unconventional position of the band at 1423 cm⁻¹ in the spectrum obtained for the recently synthesized ITO/TiO₂/P3MT, which is usually observed at approximately 1440 cm⁻¹, could indicate that the radical cation segments of the P3MT interact more strongly with the TiO₂ than observed at the interface with the P3HT. It can also be seen that the blue coloration film of the P3MT, deposited initially on the surface of the TiO₂, underwent an alteration as time progressed and was incorporated into the TiO₂ crystalline structure.

In the spectra obtained after 15 h, the band at 1423 cm⁻¹ begins to undergo a slight shift and after 97 h is positioned at 1448 cm⁻¹. Because of this strong interaction between P3MT and TiO₂ and incorporation into the TiO₂ crystalline structure, the displacement observed indicates the presence of the radical cation segment in the polymer matrix, even after 97 h.

This result shows that the TiO₂ contributes to the formation of the radical cation segment compared to previous studies,⁷ where it boosts the dication segment in the P3MT polymer matrix rather than the radical cation segment.

Figs. 4a shows the impedance magnitude and Fig. 4b Bode-phase diagrams plotted for the ITO/TiO₂/P3MT system. The low-frequency phase maxima were observed at around 0.02, 0.04 and 0.06 Hz (Fig. 4b) at the analysis times. As shown previously for the system containing P3HT, there was a partial shift of the frequency at 0.02 to those at ~0.04 and ~0.06 Hz.

As shown by the Raman spectroscopy, there was a strong interaction between the P3MT and the TiO₂ as time progressed. It must be the change of the

phase angles observed, indicating that the conduction charge-transfer process is primarily polaronic.

After 15 h, the radical cation is stabilized in the P3MT polymer matrix, confirming the results previously obtained by the Raman spectra.

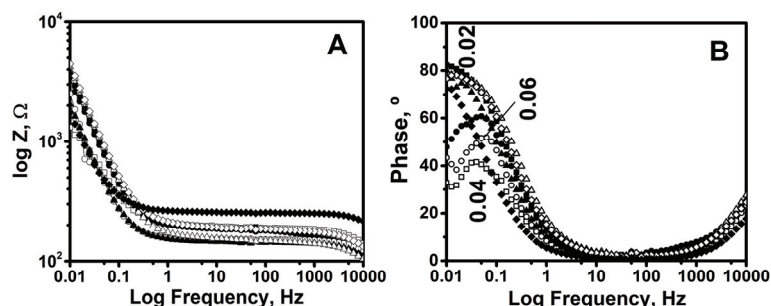


Fig. 4. a) Impedance magnitude and b) Bode-Phase diagrams at open circuit potential and constant temperature of 22 °C for the ITO/TiO₂/P3MT system. Post-synthesis analysis times were: 0 (solid square), 1 (empty square), 5 (solid circle), 10 (empty circle), 15 (solid triangle), 24 (empty triangle), 30 (empty lozenge) and 97 h (solid lozenge), after electrochemical synthesis.

Considering the need to verify the dispersion of the polymeric material on substrate surface and its incorporation into the porous structure of TiO₂, a Raman imaging was obtained from the real imaging (Fig. 5a) obtained from the confocal microscope. Filters to the TiO₂ and P3MT characteristic bands at 1448 and 1423 cm⁻¹, respectively, were used to generate a Raman imaging (Fig. 5b) of the film in the determined area (*x* and *y* axes). It was observed that regions with the accumulation of P3MT occur in the red region and in the blue region solid TiO₂ predominates. Likewise, the imaging of the thickness (*z* axis) of the ITO/TiO₂/P3MT system was obtained (Fig. 5c), where it was observed that the accumulation of P3MT occur in the red region and in the blue region TiO₂ predominates, demonstrate that the P3MT film can incorporate into the titanium oxide crystalline lattice, as previously discussed.

With the aim of modifying the effect of including P3ATs films, which underwent rearrangement in the TiO₂ crystalline structure after the deposition on TiO₂, these films at the ITO/TiO₂/PDPA interface were studied, given that the PDPA was previously examined as an inducer phase to promote the stabilization of the radical cation segments in the P3ATs polymer matrix.^{8,13}

Fig. S-2 of the Supplementary material shows the Raman spectra for the ITO/TiO₂/PDPA system, obtained at different times. After synthesis and up to 97 h, there was a predominance of the bands characteristic of the PDPA radical cation at 1202, 1320 and 1530 cm⁻¹, respectively attributed to the C–H angular deformation, the interring C–C stretching and the C–N stretching. Similarly, the

elongated band characteristic of the aromatic ring at 1607 cm^{-1} , attributed to the C–C stretching of the PDPA aromatic ring, persisted at the analysis times.¹⁵

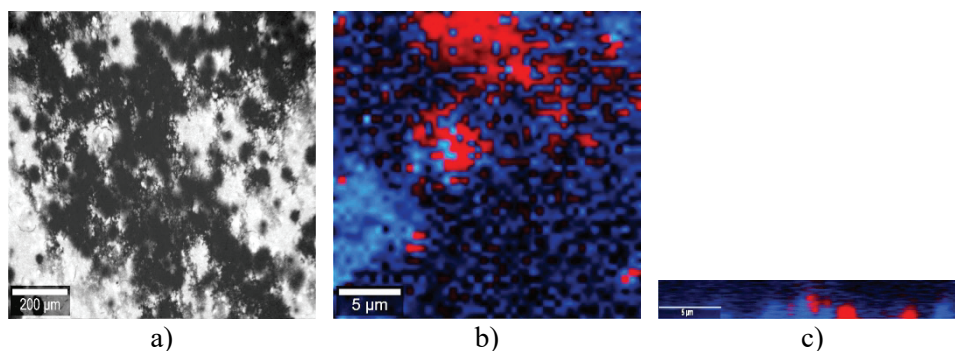


Fig. 5. Raman imaging of the ITO/TiO₂/P3MT system obtained from the confocal microscopy: a) real, b) surface and c) thickness imaging. Red regions – P3MT accumulation occurs and blue region – solid TiO₂ predominates.

According to the work of De Santana *et al.*,¹⁵ the radical cation segments exhibit an elongated absorption band between 450 and 490 nm in the UV–Vis spectra, so that the spectrum excited at 532 nm undergoes the Raman resonance intensification. Thus, the bands observed at 1202 , 1320 and 1530 cm^{-1} remained intense in the spectrum. In this study, we considered the feasibility of deconvoluting the elongated band characteristic of the aromatic ring at 1607 cm^{-1} and using it to show the relative quantities of dication, aromatic and radical cation segments present in the polymer matrix.

As shown in insets A and B of Fig. S-2, the deconvolution of the elongated band at 1607 cm^{-1} in the recently-synthesized system and after 97 h exhibited the dication, the aromatic and the radical cation segments at $1590/1562$ – 1599 , 1608 and 1621 – 1624 cm^{-1} , respectively.⁸

These findings are comparable with those of Kubota *et al.*,⁸ in which, given the same electrochemical synthesis conditions, the deposition of PDPA onto the ITO was examined. The deconvolution of the band at 1608 cm^{-1} after a period of 97 h boosted the formation of the radical cation segment, in contrast to our findings, which showed a boost in the dication segment of the film's polymer matrix, due to the presence of TiO₂ at the interface with the PDPA.

Fig. S-3 of the Supplementary materials shows the Raman spectra at different times after the electrochemical synthesis of the layered ITO/TiO₂/PDPA/P3HT system.

The spectrum after synthesis (Fig. S-3a) exhibited the bands related respectively to the PDPA radical cation and aromatic segments at 1202 , 1322 and 1527 cm^{-1} , *i.e.*, 1608 cm^{-1} and an elongated, low-intensity band at 1455 cm^{-1} , characteristic of symmetric C=C stretching of the P3HT thiophene ring.

At the different post-synthesis times, the band at 1455 cm^{-1} exhibited some variations in frequency and intensity and was more intense after 97 h. In order to understand better the behaviour of this band at 1455 cm^{-1} , this region was deconvoluted. Inset A of Fig. S-3 shows that, soon after the deposition, the frequencies showed the aromatic, the dication and the radical cation segments of the thiophene ring, respectively, at 1442 , 1458 and 1478 cm^{-1} , as in the work of Kubota *et al.*⁸ These observed shifts could probably be explained by the strong interactions between the charged layers of the PDPA and P3HT over the TiO_2 . After 97 h, the deconvolution (Fig. S-3, inset B) revealed frequencies at 1440 and 1457 cm^{-1} related to the aromatic and dication segments of the P3HT, respectively, confirming that as time progressed the dication and the aromatic segments of this system were stabilized.

Fig. S-4 of the Supplementary material is a Bode-phase diagram for the ITO/ TiO_2 /PDPA/P3HT system, revealing the phases at low and high frequency around 0.02 , 0.05 and 100 Hz , relating to charge-transfer processes at the interfaces.

In the work of Kubota *et al.*,⁸ EIS on the ITO/PDPA/P3HT system showed high instability at the analysis time, with a predominance of the elongated phase at high frequencies, indicating the stability of the dication segment. In the results obtained in the presence of TiO_2 and PDPA at the interface with P3HT, the low-frequency phase maximum at $\sim 0.02\text{ Hz}$, as shown previously for the ITO/ TiO_2 /P3HT system, alternates by $\sim 0.05\text{ Hz}$. As time progressed, the interaction of the P3HT with TiO_2 changed the phase angle as observed, indicating that the polaronic conduction charge-transfer process could be in progress. However, after 15 h, we also observed a high-frequency phase at 100 Hz , indicating a tendency to stabilize the dication segment, as observed in the Raman spectra.

Fig. S-5 of the Supplementary material shows the Raman spectra at various analysis times after the electrochemical synthesis of the ITO/ TiO_2 /PDPA/P3MT systems, prepared by layering. A discussion of these results must include the comparison with the work of De Lima *et al.*,⁷ in which deposition of P3MT onto ITO was investigated under the same electrochemical synthesis conditions. After the synthesis, the frequencies at $1204/1322$ and $1526/1607\text{ cm}^{-1}$ were observed, related respectively to the radical cation and the aromatic segments of the PDPA and a band at 1472 cm^{-1} characteristic of P3MT thiophene ring radical cation segments.

After 10 h, the band at 1472 cm^{-1} was shifted to 1458 cm^{-1} and a similar result was observed by De Lima *et al.*,⁷ although the shift was to 1457 cm^{-1} .

The band at 1472 cm^{-1} could indicate that the radical cation segments of P3MT did not strongly interact with the TiO_2 , as observed in the ITO/ TiO_2 /P3MT system. On the other hand, this result shows that the P3MT at the interface with TiO_2 in the presence of PDPA was not favourable to the formation of the radical cation segment, as observed in a previous study by De Lima *et al.*,⁷ in which the

dication segment of the P3MT polymer matrix was responsible for the band observed at 1458 cm⁻¹.

Fig. S-6 of the Supplementary material is the Bode-phase diagram for the ITO/TiO₂/PDPA/P3MT system, revealing the presence of low-frequency phase maximum around ~0.02 and ~0.05 Hz relating to the charge transfer processes at the interface.

The system as a whole exhibited high instability at the analysis time, alternating between the low-frequency phase maximum at ~0.01 Hz and the phase maximum at ~0.05 Hz, indicating a problem with stabilization of the polaronic phase in the presence of PDPA at the interface of P3MT with TiO₂. This result could also indicate a tendency to destabilize the radical cation segment in the presence of PDPA, as observed in the Raman spectra, with a predominance of spectra for bands associated with the dication.

With the aim of investigating emission associated with the radical cation segments at the polymer interface as prepared in the presence of TiO₂, photoluminescence (PL) spectra of these materials were obtained at low temperature (15 K). Next, these results were compared to the emission behaviour observed previously for P3ATs,⁶ in order to confirm the results obtained by Raman spectroscopy and EIS, in which the radical cation segments present in P3ATs were observed to interact with the TiO₂.

For the Pt/P3MT system, Bento *et al.*⁶ observed that the PL spectrum at 15 K exhibited a band at 476 nm and a shadow around 507 nm, attributed to the mixed chains formed by the aromatic and the quinone segments,¹⁶ and an intense band at 680 nm, present only at low temperature, which was associated with the boosted radical cation segments in the polymer matrix at this temperature compared to the PL spectra for the Pt/P3MT system at liquid nitrogen temperature (77 K) and at 298 K.

Fig. 6 shows the PL spectra at 15 K for the ITO/TiO₂/P3MT and ITO/TiO₂/P3HT systems under the same conditions of excitation and recording as the PL spectra previously obtained by Bento *et al.*⁶

After the deconvolution of the elongated band obtained, the emissions were observed in the PL spectra at 491, 524 and 562 nm for the ITO/TiO₂/P3MT system and at 496, 524 and 554 nm for the ITO/TiO₂/P3HT interface. Comparing the results obtained herein for the interfaces in the presence of TiO₂ with the work of Bento *et al.*,⁶ it can be inferred that the band observed at 562 nm at the TiO₂ interface with P3MT and the band at 554 nm for interfaces with P3HT could be related to the radical cation emission. This result confirms that there is an interaction between the radical cation segments of P3ATs and TiO₂, based on the drop in the intensity of the bands related to the radical cation and the shifts observed.

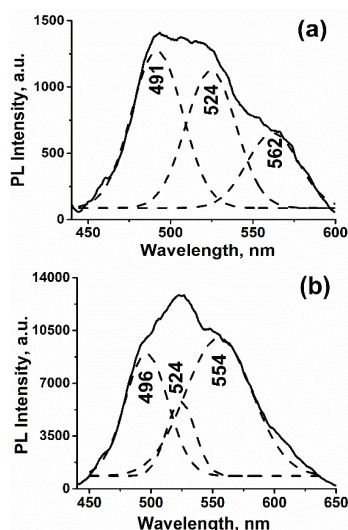


Fig. 6. PL spectra after deconvolution, obtained at a temperature of 15 K for the following systems: a) ITO/TiO₂/P3MT and b) ITO/TiO₂/P3HT.

CONCLUSION

In this study, we were able to observe the behaviour of the systems under investigation in the presence of TiO₂ and how the compounds involved behave over time at the synthesized interfaces. The presence of TiO₂ was found to result in a strong interaction among P3ATs, causing the radical cation segment to stabilize in the P3MT and P3HT polymer matrices P3HT, with good results at the post-synthesis analysis times.

After applying EIS and Raman spectroscopy to the systems under investigation, it was possible to monitor the segments present in these systems. The interface most favourable to the radical cation segment stabilization was the ITO/TiO₂/P3MT system. This system interacted most strongly with TiO₂ and combined with its crystalline structure, as well as producing an unprecedented result, not previously investigated. The radical cation was observed to stabilize in the polymer matrix, even after 97 h. The systems containing PDPA were observed to destabilize the interaction between the TiO₂ and P3ATs, to the detriment of radical cation segments at the active layer interface.

Comparing this result with those obtained by the confocal Raman technique, it was observed that the TiO₂, even though it is in excess in some regions on surface of the film formed after the deposition of the P3MT, it still coats it, even if in smaller quantities, therefore, the EIS measurements for the systems containing the P3ATs do not suffer interference from the TiO₂.

The PL results were in agreement with those obtained by Raman techniques and EIS, allowing us to recognize the interaction between the radical cation segments and TiO₂.

We consider the interfaces investigated herein to be the promising candidates for the formation of the active layer in inverted organic solar cells.

SUPPLEMENTARY MATERIAL

Additional data and information are available electronically at the pages of journal website: <https://www.shd-pub.org.rs/index.php/JSCS/article/view/12701>, or from the corresponding author on request.

Acknowledgments. We would like to express our appreciation to the Spectroscopy Laboratory (SPEC) at the PROPPG/UEL Multiuser Center. We would also like to thank the National Council for Scientific and Technological Development for its support.

ИЗВОД

ЕЛЕКТРИЧНА, ОПТИЧКА И СТРУКТУРНА КАРАКТЕРИЗАЦИЈА МЕЃУФАЗНИХ ОБЛАСТИ КОЈА САДРЖЕ ПОЛИ(3-АЛКИЛТИОФЕНЕ) (РЗАТ) И ПОЛИДИФЕНИЛАМИН НА ИТО/TiO₂: ИНТЕРАКЦИЈА ИЗМЕЂУ ПОЛИМЕРНИХ СЕГМЕНАТА РЗАТ И TiO₂

MAYARA MASAE KUBOTA¹, RICARDO VIGNOTO FERNANDES² и HENRIQUE DE SANTANA¹

¹Departamento de Química, CCE, Universidade Estadual de Londrina, Londrina, PR 86051-990, Brazil и

²Departamento de Física, CCE, Universidade Estadual de Londrina, Londrina, PR 86051-990, Brazil

У циљу испитивања могуће употребе коњугованих полимера поли(3-метилтиофена) (РЗМТ), поли(3-хексилтиофена) (РЗНТ) и полидифениламина (РДРА) за састављање активног слоја инвертованих органских соларних ћелија које формирају међуфазну област са TiO₂, а такође и да би се допринело разјашњењу која су оптичка и електронска својства активног слоја потребна за развој ове технологије, електрохемијски су направљене међуфазне области између филмова који садрже РЗМТ, РЗНТ и РДРА на индиум-калај-оксид електроди (ИТО) након што је на њега хемијски исталожен филм TiO₂. Системи који су испитивани означени су као ИТО/TiO₂/РЗМТ, ИТО/TiO₂/РДРА//РЗМТ, ИТО/TiO₂/РДРА, ИТО/TiO₂/РЗНТ и ИТО/TiO₂/РДРА/РЗНТ и карактерисани Рамановим техникама (спектроскопија и микроскопија), спектроскопијом електрохемијске импеданције (EIS) и фотолуминисценцијом (PL). У овој студији су ароматични, семихинонски и хинонски сегменти у полимерним матрицама РЗАТ и РДРА на наведеним границама фаза карактерисани помоћу Раманове спектроскопије и EIS и поређени са филмовима њихових хомополимера. Раманове технике показују да се филм РЗМТ може уградити у кристалну решетку TiO₂. Утврђено је да системи који садрже РЗМТ или РЗНТ остварују јаку интеракцију са TiO₂ стабилишући сегменте катјонских радикала РЗАТ, док присуство РДРА дестабилизује ову интеракцију. Приказани резултати, допуњени нискотемпературним (15 К) PL спектром, показали су смањење интензитета и померај траке повезане с емисијом катјонских радикала, што је запажено када у испитиваном систему није био присутан TiO₂.

(Примљено 25. новембра 2023, ревидирано 24. јануара, прихваћено 3. марта 2024)

REFERENCES

1. M. Abdallaoui, N. Sengouga, A. Chala, A. F. Meftah, A. M. Meftah, *Opt. Mater.* **105** (2020) 109916 (<https://doi.org/10.1016/j.optmat.2020.109916>)
2. S. K. Hau, H.-L. Yip, A. K.-Y. Jen, *Polym. Rev.* **50** (2010) 474 (<https://doi.org/10.1080/15583724.2010.515764>)

3. D. W. Zhao, S. T. Tan, L. Ke, P. Liu, A. K. K. Kyaw, X. W. Sun, G. Q. Lo, D. L. Kwong, *Sol. Energy Mater. Sol. Cells* **94** (2010) 985 (<https://doi.org/10.1016/j.solmat.2010.02.010>)
4. C. J. Brabec, *Sol. Energy Mater. Sol. Cells* **83** (2004) 273 (<https://doi.org/10.1016/j.solmat.2004.02.030>)
5. A. D. Batista, W. Renzi, J. L. Duarte, H. De Santana, *J. Electron. Mater.* **47** (2018) 6403 (<https://doi.org/10.1007/s11664-019-07268-6>)
6. D. C. Bento, E. C. R. Maia, T. N. M. Cervantes, R. V. Fernandes, E. Di Mauro, E. Laureto, M. A. T. Da Silva, J. L. Duarte, I. F. L. Dias, H. De Santana, *Synth. Met.* **162** (2012) 2433 (<https://doi.org/10.1016/j.synthmet.2012.12.006>)
7. J. H. C. De Lima, D. F. Valezi, A. D. Batista, D. C. Bento, H. De Santana, *J. Mater. Sci.: Mater. Electron.* **29** (2018) 6511 (<https://doi.org/10.1007/s10854-018-8633-z>)
8. M. M. Kubota, H. De Santana, *J. Electron. Mater.* **50** (2021) 1167 (<https://doi.org/10.1007/s11664-020-08685-8>)
9. M.R. Hoffmann, S.T. Martin, W.Y. Choi, D.W. Bahnemann, *Chem. Rev.* **95** (1995) 69 (<https://doi.org/10.1021/cr00033a004>)
10. M.K. Nazeeruddin, A. Kay, I. Rodicio, R. Humphry-Baker, E. Muller, P. Liska, N. Vlachopoulos, M. Grätzel, *J. Am. Chem. Soc.* **115** (1993) 6382 (<https://doi.org/10.1021/ja00067a063>)
11. S. Quillard, G. Louarn, J. P. Buisson, S. Lefrant, J. Masters, A. G. MacDiarmid, *Synth. Met.* **50** (1992) 525 ([https://doi.org/10.1016/0379-6779\(92\)90208-Z](https://doi.org/10.1016/0379-6779(92)90208-Z))
12. X. Feng, X. Wang, *Thin Solid Films* **519** (2011) 5700 (<https://doi.org/10.1016/j.tsf.2011.03.043>)
13. M. Baibarac, M. Lapkowski, A. Pron, S. Lefrant, I. Baltog, *J. Raman Spectrosc.* **29** (1998) 825 ([https://doi.org/10.1002/\(SICI\)1097-4555\(199809\)29:9<825::AID-JRS309>3.0.CO;2-2](https://doi.org/10.1002/(SICI)1097-4555(199809)29:9<825::AID-JRS309>3.0.CO;2-2))
14. G. Louarn, J. Y. Mevellec, J. P. Buisson, S. Lefrant, *Synth. Met.* **55-57** (1993) 587 ([https://doi.org/10.1016/0379-6779\(93\)90996-A](https://doi.org/10.1016/0379-6779(93)90996-A))
15. H. De Santana, M. L. A. Temperini, J. C. Rubim, *J. Electroanal. Chem.* **356** (1993) 145 ([https://doi.org/10.1016/0022-0728\(93\)80516-K](https://doi.org/10.1016/0022-0728(93)80516-K))
16. E. M. Thérézio, J. L. Duarte, E. Laureto, E. Di Mauro, I. F. L. Dias, A. Marletta, H. De Santana, *J. Phys. Org. Chem.* **24** (2011) 640 (<https://doi.org/10.1002/poc.1802>).